Self-Assembly of Multicomponent Structures In and Out of Equilibrium

Stephen Whitelam,[1,*] Rebecca Schulman,[2,†] and Lester Hedges[1]

[1]*Molecular Foundry, Lawrence Berkeley National Laboratory, 1 Cyclotron Road, Berkeley, California 94720, USA*
[2]*Chemical and Biomolecular Engineering and Computer Science, Johns Hopkins University, 3400 N Charles Street, Baltimore, Maryland 21218, USA*

(Received 17 April 2012; revised manuscript received 9 October 2012; published 28 December 2012)

Theories of phase change and self-assembly often invoke the idea of a ''quasiequilibrium,'' a regime in which the nonequilibrium association of building blocks results nonetheless in a structure whose properties are determined solely by an underlying free energy landscape. Here we study a prototypical example of multicomponent self-assembly, a one-dimensional fiber grown from red and blue blocks. We find that if the equilibrium structure possesses compositional correlations different from those characteristic of random mixing, then it cannot be generated without error at any finite growth rate: there is no quasiequilibrium regime. However, by exploiting dynamic scaling, structures characteristic of equilibrium at one point in phase space can be generated, without error, arbitrarily far from equilibrium. Our results, supported by mean-field theory in higher dimensions, thus suggest a ''nonperturbative'' strategy for multicomponent self-assembly in which the target structure is, by design, not the equilibrium one.

DOI: 10.1103/PhysRevLett.109.265506 PACS numbers: 81.16.Dn, 05.20.−y, 81.16.Fg

Many theories of phase change and self-assembly place at their heart the idea that dynamical trajectories follow low-lying paths on the free energy landscape connecting reactants and products [1–11]. This idea underpins rate equation theories [1,3–5], classical nucleation theory [1,2] and density functional theory [7–11]—which assume that a structure's morphology is determined by minima or low-lying paths on the underlying free energy landscape–and the conjecture of Stranski and Totomanow [12], which states that a system, confronted by a set of free energy barriers, will evolve by crossing the lowest of them. These formal statements reflect the intuition that one can generate structures characteristic of equilibrium using a sufficiently ''mild'' nonequilibrium protocol. Many one-component systems indeed assemble in quasiequilibrium [10,11,13–15] if they are not deeply supercooled [16,17] or plagued by slow particle dynamics [18]. However, a substantial literature suggests that *multicomponent* self-assembly is susceptible to kinetic factors even under conditions of weak driving [19–26]. For instance, the Stranski-Totomanow assumption breaks down in a particular case of simulated binary colloid nucleation, where sluggish interspecies mixing prevents nuclei from establishing compositional equilibrium [27,28]. Also, binary crystals have been observed in simulation and experiment to grow out of compositional equilibrium, even under conditions mild enough to produce morphologically ordered structures [24–26]. To describe such assembly theoretically, one must account for dynamical processes that drive a system away from low-lying paths on the free energy landscape [19–23,28–31]. On a practical level, one can ask under what conditions can precisely defined multicomponent structures be self-assembled, if evolution even near a phase boundary leads to a structure not characteristic of the equilibrium one?

Here we study this question within a prototypical example of multicomponent self-assembly. We apply simulation and quantitatively accurate analytic theory to the fluctuating growth of a model lattice-based fiber built from red and blue blocks. We show that when compositional correlations of the equilibrium structure are not equal to those of the randomly mixed material incident on the fiber, the former cannot be generated at a finite rate of growth. Moreover, structures that assemble even close to the phase boundary can be very different from equilibrium ones. This absence of a quasiequilibrium regime occurs despite the fact that fibers near the phase boundary grow in a ''quasireversible'' manner, displaying many unbinding events. However, by exploiting dynamic scaling connecting equilibrium and nonequilibrium parameter manifolds, defined structures can be generated without error arbitrarily far from equilibrium. The failure of a widely made assumption for perhaps the simplest example of compositionally inhomogeneous self-assembly confirms the need for the development of dynamical theories [23,26,30,32–35] in order to describe the self-assembly of multicomponent structures, and challenges the idea that the equilibrium structure is the natural target for multicomponent self-assembly.

Model.—We consider a one-dimensional stochastic growth process in which a fiber is built from red and blue blocks [Fig. 1(a)]. We add blocks to the right-hand end of the fiber with rate c (concentration). Added blocks are blue with probability p_{blue}, and red otherwise. We allow the rightmost block to detach from the fiber with rate $e^{-\beta\epsilon_i}$, which depends on the nature of the rightmost bond of the fiber. Nearest-neighboring blocks of the same color interact with energy $-\epsilon_i = -\epsilon_s$, while the red-blue interaction is $-\epsilon_d$ (we set $\beta = 1$ throughout). We implemented this stochastic process in simulations using a kinetic Monte Carlo procedure

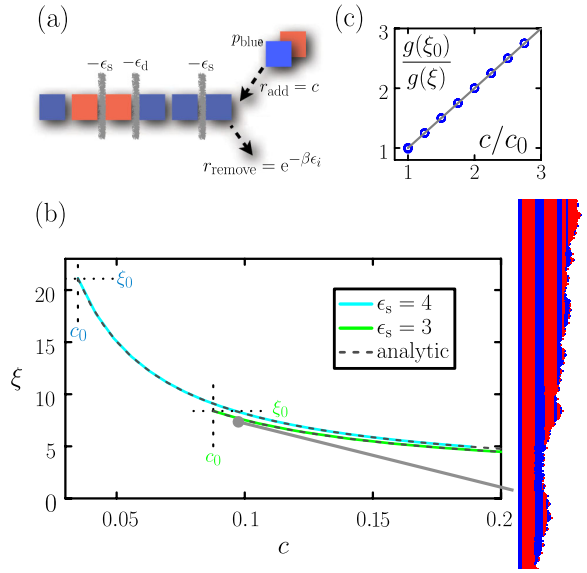

FIG. 1 (color online). Fiber structures depend sensitively upon preparation conditions. (a) Schematic of fiber energetics and growth rates. (b) Domain lengths ξ of dynamically generated fibers of given energy scales ϵ_s (simulations: solid lines, theory: dashed lines) are less than the corresponding equilibrium domain lengths ξ_0 (horizontal dashed lines) for all points past the phase boundary $c = c_0$ (vertical dashed lines). This breakdown of the quasiequilibrium assumption reflects the conflict between compositional correlations of unassembled material and the equilibrium structure, and occurs despite the fact that fibers close to the phase boundary grow in a quasireversible way. (c) Simulation data can be collapsed onto a master curve, summarizing the continuous variation of the scaled domain length $g(\xi) \equiv \xi(\xi-2)/(\xi-1)$ with concentration c.

[36,37]: we removed the terminal block with probability $p_{\text{remove}} = 1/(1 + ce^{\beta\epsilon_i})$, where $i = s$ or d as appropriate, and otherwise added a block to the fiber end. This idealized fluctuating protocol captures the key kinetic constraint imposed upon the physical process of 3D assembly: material can be removed only from the interface between a structure and its environment [26]. By considering a lattice model in which complications of morphology and the possibility of internal block rearrangements are suppressed, we can explore directly how this constraint affects pattern generation. Imposing this constraint results immediately in important qualitative behaviors seen also in 3D systems; we shall show how analysis of these behaviors suggests an unconventional and potentially powerful strategy for self-assembly.

The "equilibrium" we consider is the one often imagined in theories of self-assembly, corresponding to minimization of the free energy of a structure of fixed size [10,11,13,15]. Such an equilibrium is achieved by our dynamical protocol in the limit of a large number of binding and unbinding events per site [38]: a key question is how the structure generated at a finite rate of growth compares to the equilibrium one. The energetics of a fiber of fixed size is that of the 1D Ising model [39,40], with Hamiltonian $\mathcal{H} = -J\sum_i S_i S_{i+1} - h\sum_i S_i$. Here the spin variable $S_i = \pm 1$ describes a blue ($S_i = 1$) or red ($S_i = -1$) block; the coupling $J = (\epsilon_s - \epsilon_d)/2$ is the penalty for domain wall (red-blue bond) creation; and the magnetic field $h = -\ln(1/p_{\text{blue}} - 1)/2$ describes the bias for blue blocks over red ones. Here we add red and blue blocks with equal likelihood, i.e., $p_{\text{blue}} = 1/2$, equivalent to $h = 0$. In this case the equilibrium structure of a fiber consists of equal proportions of red and blue blocks arranged into domains whose lengths ℓ occur with probability $\rho_0(\ell) = (\xi_0 - 1)^{-1} \exp[\ell \ln(1 - \xi_0^{-1})]$. Here, $\xi_0 = 1 + \exp(2\beta J)$ is the mean domain length in equilibrium.

Results.—We carried out dynamic simulations for the choice $\epsilon_d = 1$ and a range of values of $\epsilon_s > \epsilon_d$ (for which $\xi_0 > 2$). For each set of energetic parameters we considered a range of concentrations c. When $c < c_0 = 2/(e^{\beta\epsilon_s} + e^{\beta\epsilon_d})$ the fiber does not grow. When $c = c_0$ the drift velocity of the fiber, averaged over distances greater than a typical domain length, is exactly zero. The fiber therefore "grows" only by diffusion of its rightmost end. When $c > c_0$ the fiber grows with nonzero drift velocity. We therefore consider the concentration c_0 to define the "phase boundary" between nonassembly and assembly. We stopped dynamic simulations when a fiber of length $L = 2.5 \times 10^4$ blocks was generated. We performed 10^4 simulations for each concentration considered, except at the phase boundary, where the diffusive growth of a fiber was slow; there, we generated about 200 fibers for each set of conditions. For each ensemble of fibers we measured the probability distribution of domain lengths $\rho(\ell) = n(\ell)/\sum_{\ell=1}^{L} n(\ell)$, where $n(\ell)$ is the number of occurrences of domain length ℓ across all simulations at given thermodynamic conditions. These distributions were always exponential (Fig. S1 in the Supplemental Material [41]) with a mean ξ depending on all three parameters c, ϵ_s and ϵ_d. This mean is shown in Fig. 1(b) for two choices of ϵ_s. At the phase boundary the equilibrium structure is generated. For all points past the phase boundary, the dynamic domain length ξ is less than the equilibrium one ξ_0, despite the fact that fiber growth close to the phase boundary is highly fluctional, exhibiting many unbinding events [Fig. 1(b), space-versus-time snapshot at right]. Moreover, fiber structures are exquisitely sensitive to preparation conditions, and change continuously with supersaturation.

Analytic theory reveals that this sensitivity is an inevitable consequence of the different compositional statistics of the equilibrium structure and unassembled material. Consider defect variables $\eta_i \equiv S_i S_{i+1}$, where $\eta_i = 1$ describes a bulk (same-color) bond and $\eta_i = -1$ is a defect (unlike-color) one. Let $\phi \equiv [(\eta_i + 1)/2]$ be the likelihood that a given bond is a bulk one, where the average $[\cdot]$ is taken over many realizations of the dynamics. Enumeration of basic microscopic processes (see the Supplemental Material [41]) implies a drift velocity for bulk domains

$$v_{\text{bulk}} = c/2 - \phi e^{-\beta\epsilon_s}, \quad (1)$$

and a drift velocity for the fiber

$$v_{\text{fiber}} = c - \phi e^{-\beta\epsilon_s} - (1-\phi)e^{-\beta\epsilon_d}. \quad (2)$$

At the phase boundary, where $v_{\text{bulk}} = v_{\text{fiber}} = 0$, Eqs. (1) and (2) give the equilibrium bulk fraction $\phi_0 = 1/(1 + e^{\beta(\epsilon_d - \epsilon_s)})$, and the equilibrium concentration $c_0 = 2/(e^{\beta\epsilon_d} + e^{\beta\epsilon_s})$. ξ_0 and c_0 are given by horizontal and vertical dotted lines on Fig. 1(b). Fiber *dynamics* can be solved by requiring $v_{\text{bulk}}/v_{\text{fiber}} = \phi$, yielding

$$\phi = \frac{c/2 - \phi e^{-\beta\epsilon_s}}{c - \phi e^{-\beta\epsilon_s} - (1-\phi)e^{-\beta\epsilon_d}}. \quad (3)$$

This equation is straightforwardly solved (see Eq. S1 in the Supplemental Material [41]) for the domain length $\xi = 1/(1-\phi)$, and we plot this solution as grey dashed lines in Fig. 1(b). The agreement with simulation is good, confirming the sensitivity of fiber structure to method of preparation. Moreover, the structure of Eq. (3) reveals the origin of this sensitivity. Its large-c limit returns the domain length characteristic of random mixing, $\xi_\infty = 2$, which is in general unequal to the equilibrium domain length ξ_0. At the phase boundary, the balance of c-dependent and -independent terms in Eq. (3) is such that bulk domains are generated at a rate characteristic of equilibrium. For finite supersaturation, however, the statistics of the fiber begins to reflect the statistics of random mixing: Eq. (3) can be expanded in small deviations $\delta c \equiv c - c_0$ from the phase boundary to yield

$$\xi - \xi_0 \approx -\frac{\xi_0}{c_0}\frac{(\xi_0 - 2)(\xi_0 - 1)}{\xi_0(\xi_0 - 2) + 2}\delta c. \quad (4)$$

Thus fiber structure is a continuous function of concentration, and the dynamic correlation length is less than the equilibrium one for *any* concentration $c > c_0$. Equivalently, structures generated at finite growth rate always sit above the minimum of the free energy landscape (Fig. S2 in the Supplemental Material [41]).

Comparison of simulation and analytic theory thus reveals that a fiber's dynamically generated structure can be understood by considering only the relative *net* rates of bulk domain generation and fiber elongation. Although the relaxation time for a given site is governed by the number of times the fiber end diffuses back and forth across it, with sites far from the fiber end being "locked in" [26], the structures generated by our fluctuating simulation protocol are explained solely by the competition between the compositional statistics of equilibrium and random mixing. The departure from quasiequilibrium follows from this competition enacted at finite drift velocity, where randomness associated with unassembled material trumps correlation induced by block binding energies. The rate of this departure, given to lowest order by Eq. (4), has practical consequences for the design of fiber patterns. For target structures mimicking conventional binary crystals, having $\xi_0 \approx 1$, the conventional "perturbative" scheme of growing some small distance δc from the phase boundary leads to a structure with few errors, whose compositional correlations are numerically close to the target one (Fig. S3 in the Supplemental Material [41]). We note that simulated 3D binary crystals can likewise be grown close to compositional equilibrium [26]. However, when the desired target possesses long range compositional correlations, growth even close to the phase boundary results in many errors (Fig. S4 in the Supplemental Material [41]). Similar predominance of kinetics is seen in the growth of segregated binary assemblies [24,25].

The perturbative method of self-assembly thus becomes increasingly unattractive as the compositional correlations of the target structure become increasingly complex. Here we propose an alternative nonperturbative approach. Our model's dynamics, Eq. (3), can be cast in the scaling form

$$c/c_0 = g(\xi_0)/g(\xi), \quad (5)$$

where $g(\xi) \equiv \xi(\xi - 2)/(\xi - 1)$ is a scaled correlation length. This expression reveals that the results of dynamic simulations can be collapsed onto a straight line connecting a manifold of nonequilibrium conditions with an equilibrium point at (1, 1). We verified this collapse for a range of simulations carried out at 40 different phase points [Fig. 1(c)] whose values of ϵ_s ranged from 2 to 6. The nature of the master curve demonstrates that no fiber having $\xi = \xi_0$ can be generated anywhere past the phase boundary $c = c_0$, and emphasizes the sensitivity of structure ξ to preparation condition c. But it also describes a useful connection between patterns in and out of equilibrium. It can be rearranged to read

$$c = \frac{2(\xi - 1)}{\xi(\xi - 2)}(e^{-\beta\epsilon_d} - e^{-\beta\epsilon_s}), \quad (6)$$

revealing that structures of identical ξ can be generated on a manifold of parameters c, ϵ_s, and ϵ_d, regardless of distance to the phase boundary. We illustrate this manifold in Fig. 2. ξ is constant along the displayed contour lines. Simulations verify this prediction (Fig. S5 in the Supplemental Material [41]): structures generated dynamically at the circles on each contour line are indistinguishable. However, fiber generation changes from being purely diffusive (and very slow) at the phase boundary, to being nearly irreversible (and very fast) far from it, illustrated by the space-time trajectories shown (see also Fig. S5 in the Supplemental Material [41]). Moving rightwards along contours, the generated structures lie increasingly far from the equilibrium one for the corresponding energetic parameters (Fig. 2, inset); nonetheless, structures characteristic of equilibrium at a particular point on the phase boundary can be generated by a continuum of nonequilibrium protocols away from it. In this sense, equilibrium structures can be grown, error-free, arbitrarily far from equilibrium.

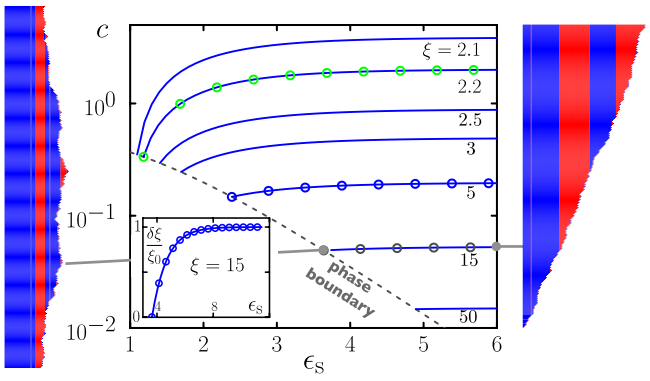

FIG. 2 (color online). Defined structures can be grown in equilibrium and far from it. Along each contour, defined by Eq. (6), identical structures can be generated by reversible dynamic protocols (at the phase boundary), or nearly irreversible ones (far from the phase boundary), illustrated by the simulation snapshots. Inset: distance $(\xi_0 - \xi)/\xi_0$ to equilibrium of structures generated along the $\xi = 15$ contour (circles: simulation data; line: analytic results).

Conclusions.—Compositionally inhomogeneous structures are found abundantly in biology [42,43], and are increasingly the target of designed self-assembly processes [25,44–48]. However, it is increasingly clear that in order to ensure the self-assembly of a desired multicomponent structure, specification of a free energy surface [49,50] is in general not sufficient [19–27]. Instead, explicit accounting of how microscopic dynamics [51] select assembly pathways [52,53] is required. Here we have shown how to exploit directly the relationships between the rates of elementary microscopic processes in order to generate a structure of defined composition, *regardless* of whether that composition is the underlying equilibrium one. Although the model we have studied is highly simplified, lacking, e.g., the cooperativity characteristic of crystals in higher dimensions, it shares two important qualitative features with real systems. First, a mismatch in compositional statistics between randomly mixed particles and those of the desired structure means that any attempt to assemble the equilibrium structure using a nonequilibrium protocol incurs errors. When this mismatch is small, errors are few (Fig. S3 in Ref. [41] and Ref. [26]); when this mismatch is large, errors are numerous (Fig. 1, Fig. S4 in Ref. [41], and Refs. [24,25]). Second, the dynamic scaling exhibited by our model, which permits the precise far-from-equilibrium assembly strategy we have described, is strikingly reminiscent of data collapse seen in segregated binary structure growth. There, an effective compositional order parameter scales with effective crystal growth velocity [25] (in a regime in which crystals are *morphologically* ordered). Mean-field theory (see the Supplemental Material [41]) indicates that these similarities are not accidental, but exist because the dynamic behaviors that allow the far-from-equilibrium assembly strategy in the fiber model survive in higher-dimensional systems possessing thermodynamic phase transitions at finite temperature. Our results therefore suggest the possibility of doing with real systems as as we have done within our model: design compositionally ordered structures in equilibrium, and assemble them far from it.

We thank Tom Haxton, Rob Jack, and David Sivak for discussions. S. W. was supported by the Director, Office of Science, Office of Basic Energy Sciences, of the U.S. Department of Energy under Contract No. DE-AC02-05CH11231. R. S. was supported by Johns Hopkins. L. O. H. was supported by the Center for Nanoscale Control of Geologic CO_2, a U.S. D.O.E. Energy Frontier Research Center, under Contract No. DE-AC02-05CH11231.

*swhitelam@lbl.gov
†rschulm3@jhu.edu

[1] R. Becker and W. Döring, Ann. Phys. (N.Y.) **416**, 719 (1935).
[2] M. Volmer and A. Weber, Z. Phys. Chem. **119**, 277 (1926).
[3] K. Binder and D. Stauffer, Adv. Phys. **25**, 343 (1976).
[4] A. Zlotnick, J. Mol. Biol. **241**, 59 (1994).
[5] D. Endres and A. Zlotnick, Biophys. J. **83**, 1217 (2002).
[6] M. J. Uline and D. S. Corti, Phys. Rev. Lett. **99**, 076102 (2007).
[7] J. Hansen and I. McDonald, *Theory of Simple Liquids* (Academic Press, New York, 2006).
[8] R. Evans, Adv. Phys. **28**, 143 (1979).
[9] J. F. Lutsko, Adv. Chem. Phys. **144**, 1 (2010).
[10] Y. C. Shen and D. W. Oxtoby, Phys. Rev. Lett. **77**, 3585 (1996).
[11] J. F. Lutsko and G. Nicolis, Phys. Rev. Lett. **96**, 046102 (2006).
[12] I. N. Stranski and D. Totomanov, Z. Phys. Chem. **163**, 399 (1933).
[13] P. R. Wolde and D. Frenkel, Phys. Chem. Chem. Phys. **1**, 2191 (1999).
[14] R. Sear, J. Phys. Condens. Matter **19**, 033101 (2007).
[15] P. R. Wolde and D. Frenkel, Science **277**, 1975 (1997).
[16] M. Hagan, O. Elrad, and R. Jack, J. Chem. Phys. **135**, 104 115 (2011).
[17] J. Grant and R. L. Jack, Phys. Rev. E **85**, 021112 (2012).
[18] L. Hedges and S. Whitelam, J. Chem. Phys. **135**, 164 902 (2011).
[19] K. Kremer, J. Aerosol Sci. **9**, 243 (1978).
[20] D. Stauffer, J. Aerosol Sci. **7**, 319 (1976).
[21] H. Trinkaus, Phys. Rev. B **27**, 7372 (1983).
[22] J. Schmelzer, A. Abyzov, and J. Möller, J. Chem. Phys. **121**, 6900 (2004).
[23] J. Schmelzer, J. Schmelzer, Jr., and I. Gutzow, J. Chem. Phys. **112**, 3820 (2000).
[24] R. Scarlett, J. Crocker, and T. Sinno, J. Chem. Phys. **132**, 234 705 (2010).
[25] A. Kim, R. Scarlett, P. Biancaniello, T. Sinno, and J. Crocker, Nat. Mater. **8**, 52 (2008).
[26] R. Scarlett, M. Ung, J. Crocker, and T. Sinno, Soft Matter **7**, 1912 (2011).

[27] E. Sanz, C. Valeriani, D. Frenkel, and M. Dijkstra, Phys. Rev. Lett. **99**, 055501 (2007).
[28] B. Peters, J. Chem. Phys. **131**, 244 103 (2009).
[29] K. A. Fichthorn and W. H. Weinberg, J. Chem. Phys. **95**, 1090 (1991).
[30] J. Lutsko, J. Chem. Phys. **135**, 161 101 (2011).
[31] J. Lutsko, J. Chem. Phys. **136**, 034509 (2012).
[32] U. Marconi and P. Tarazona, J. Chem. Phys. **110**, 8032 (1999).
[33] J. Fraaije, J. Chem. Phys. **99**, 9202 (1993).
[34] B. Peters, J. Chem. Phys. **135**, 044107 (2011).
[35] S. Corezzi, C. De Michele, E. Zaccarelli, P. Tartaglia, and F. Sciortino, J. Phys. Chem. B **113**, 1233 (2009).
[36] A. Bortz, M. Kalos, and J. Lebowitz, J. Comput. Phys. **17**, 10 (1975).
[37] D. Gillespie, J. Comput. Phys. **22**, 403 (1976).
[38] This protocol is unlike crystal growth done using, say, Metropolis Monte Carlo dynamics [26], because the latter obeys detailed balance with respect to an underlying Hamiltonian. However, it is similar in the sense that both protocols achieve equilibrium only in the limit of zero growth rate.
[39] J. Binney, N. Dowrick, A. Fisher, and M. Newman, *The Theory of Critical Phenomena* (Clarendon Press, Oxford, 1992).
[40] D. Chandler, *Introduction to Modern Statistical Mechanics* (Oxford University Press, New York, 1987).
[41] See Supplemental Material at http://link.aps.org/supplemental/10.1103/PhysRevLett.109.265506 for details of analytic theory and additional simulation results.
[42] D. A. Brown and E. London, Annu. Rev. Cell Dev. Biol. **14**, 111 (1998).
[43] Y. Takahashi, A. Ueno, and H. Mihara, Chembiochem **3**, 637 (2002).
[44] T. Kato, Science **295**, 2414 (2002).
[45] H. A. Behanna, J. J. M. Donners, A. C. Gordon, and S. I. Stupp, J. Am. Chem. Soc. **127**, 1193 (2005).
[46] S. Glotzer and M. J. Solomon, Nat. Mater. **6**, 557 (2007).
[47] R. D. Barish, R. Schulman, P. W. K. Rothemund, and E. Winfree, Proc. Natl. Acad. Sci. U.S.A. **106**, 6054 (2009).
[48] K. Velikov, C. Christova, R. Dullens, and A. van Blaaderen, Science **296**, 106 (2002).
[49] Z. Zhang and S. C. Glotzer, Nano Lett. **4**, 1407 (2004).
[50] M. P. Brenner and S. Hormoz, Proc. Natl. Acad. Sci. U.S.A. **108**, 5193 (2011).
[51] R. Schulman and E. Winfree, SIAM J. Comput. **39**, 1581 (2009).
[52] S. Pandey, M. Ewing, A. Kunas, N. Nguyen, D. H. Gracias, and G. Menon, Proc. Natl. Acad. Sci. U.S.A. **108**, 19 885 (2011).
[53] E. Jankowski and S. C. Glotzer, Soft Matter **8**, 2852 (2012).